

## RESEARCH ARTICLE

# Tumor stemness and immune infiltration synergistically predict response of radiotherapy or immunotherapy and relapse in lung adenocarcinoma

Hongjie Shi<sup>1</sup> | Linzhi Han<sup>2</sup> | Jinping Zhao<sup>1</sup> | Kaijie Wang<sup>1</sup> | Ming Xu<sup>1</sup> | Jiajun Shi<sup>1</sup> | Zhe Dong<sup>1</sup> 

<sup>1</sup>Department of Thoracic and Cardiovascular Surgery, Zhongnan Hospital of Wuhan University, Wuhan, China

<sup>2</sup>Department of Radiation and Medical Oncology, Zhongnan Hospital of Wuhan University, Wuhan, China

## Correspondence

Zhe Dong, Department of Thoracic and Cardiovascular Surgery, Zhongnan Hospital of Wuhan University, Shuiguohu street, Wuchang District, Wuhan 430071, China.  
Email: zn002747@whu.edu.cn

## Funding information

This study did not receive any specific grant from funding agencies in the public, commercial, or not-for-profit sectors.

## Abstract

Cancer stem cells (CSCs) have been shown to accelerate tumor recurrence, radiotherapy, and chemotherapy resistance. Immunotherapy is a powerful anticancer treatment that can significantly prolong the overall survival of patients with lung adenocarcinoma (LUAD). However, little is known about the function of genes related to tumor stemness and immune infiltration in LUAD. After integrating the tumor stemness index based on mRNA expression (mRNAsi), immune score, mRNA expression, and clinical information from the TCGA database, we screened 380 tumor stemness and immune (TSI)-related genes and constructed a five TSI-specific-gene (CPS1, CCR2, NT5E, ANLN, and ABCC2) signature (TSISig) using a machine learning method. Survival analysis indicated that TSISig could stably predict the prognosis of patients with LUAD. Comparison of mRNAsi and immune score between high- and low-TSISig groups suggested that TSISig characterized tumor stemness and immune infiltration. In addition, enrichment of immune subpopulations showed that the low-TSISig group held more immune subpopulations. GSEA revealed that TSISig had a strong association with the cell cycle and human immune response. Further analysis revealed that TSISig not only had a good predictive ability for prognosis but could also serve as an excellent predictor of tumor recurrence and response to radiotherapy and immunotherapy in LUAD patients. TSISig might regulate the development of LUAD by coordinating tumor stemness and immune infiltration. Finally, a connectivity map (CMap) analysis demonstrated that the HDAC inhibitor could target TSISig.

## KEYWORDS

immune infiltration, immunotherapy, lung adenocarcinoma (LUAD), radiotherapy, tumor recurrence, tumor stemness

Hongjie Shi and Linzhi Han have contributed equally to this work.

This is an open access article under the terms of the Creative Commons Attribution-NonCommercial-NoDerivs License, which permits use and distribution in any medium, provided the original work is properly cited, the use is non-commercial and no modifications or adaptations are made.

© 2021 The Authors. *Cancer Medicine* published by John Wiley & Sons Ltd.

## 1 | INTRODUCTION

Lung cancer has been one of the most diagnosed and lethal cancers worldwide in the past decade. In 2018, newly diagnosed lung cancer accounted for 12% of all human cancers, with 18.4% of the total number of deaths.<sup>1,2</sup> Lung adenocarcinoma (LUAD) is the most common tissue subtype of lung cancer, accounting for almost half of all lung cancers.<sup>3</sup> Although surgery, chemotherapy, and radiotherapy have greatly improved the survival of patients with LUAD, the prognosis of patients with LUAD is still poor.<sup>4</sup> Immunotherapy is a popular treatment currently. It could greatly improve the anti-cancer ability of patients.<sup>5</sup> However, current clinical trials indicate that not all patients benefited from immunotherapy. Cancer stem cells (CSCs) have been shown to play an important role in tumor recurrence, radiotherapy, and chemotherapy resistance with the tumor's ability of self-renewal, differentiation, and proliferation.<sup>6,7</sup> Interestingly, some studies have suggested that there might exist a class of genes that promote cancer development by maintaining tumor stemness and suppressing immune infiltration.<sup>8-12</sup> Our study aimed to screen tumor stemness and immune infiltration (TSI)-related genes and explore the underlying functions and mechanisms based on TCGA and GEO databases, which might provide a novel and potential signature for LUAD treatment.

In this study, we classified patients with LUAD into high/low-mRNasi groups and high/low-immune score groups according to the optimal survival tipping points. Differentially expressed genes (DEGs) between the high-mRNasi-low-immune score group and others were identified as TSI-specific genes. Then, a five-gene signature (of CPS1, CCR2, NT5E, ANLN, and ABCC2) based on TSI-specific genes (TSISig) was constructed. All the five TSI-specific genes could serve as independent prognostic factors in LUAD. The comparison of mRNasi and immune score between high- and low-TSISig and GSEA analyses suggested that TSISig could characterize tumor stemness and immune infiltration well. Finally, authentication of clinical effects showed that TSISig could be regarded as an excellent predictor of prognosis, tumor relapse, and response to radiotherapy and immunotherapy in LUAD. HDAC inhibitors could serve as targeted inhibitors of TSISig according to CMap analysis.

## 2 | MATERIALS AND METHODS

### 2.1 | LUAD datasets and preprocessing

The workflow chart is displayed in Figure S1. RNA-sequencing data (FPKM values) and clinical annotations

of LUAD patients were obtained from The Cancer Genome Atlas (TCGA; <https://portal.gdc.cancer.gov>) and the Gene Expression Omnibus (GEO; <http://www.ncbi.nlm.nih.gov/geo>). A study by Maciej Wiznerowicz et al. generated tumor stemness index based on mRNA expression (mRNAsi) of 512 patients with LUAD.<sup>13</sup> They used one-class logistic regression machine-learning algorithm (OCLR) for multi-platform analyses of transcriptome, methylome, and transcription factor binding sites and finally stemness indices was obtained. After excluding patients with a follow-up period of less than 30 d, 484 patients with LUAD and their mRNA expression and somatic mutation data were selected from the TCGA database. ESTIMATE (Estimation of STromal and Immune cells in Malignant Tumour tissues using Expression data) is a new algorithm that could infer the immune and stromal scores of samples based on immune or stromal cell-specific expression genes.<sup>14</sup> Here, R package “estimate” was performed to calculate the immune score of these samples. Among the 484 patients, the 49 receiving radiotherapy had records of clinical outcomes. Four external validation sets downloaded from GEO based on three different platforms were used to validate our gene signature (GSE31210 and GSE30219 profiled by the Affymetrix HG-U133\_Plus 2.0 platform, GSE72094 profiled by Rosetta/Merck Human RSTA Custom Affymetrix 2.0 microarray platform, and GSE36471 profiled by Agilent-UNC-custom-4X44K platform). After examining the corresponding survival information of the four datasets, a total of 807 LUAD patients (GSE31210: 226 LUAD patients, GSE30219: 83 LUAD patients, GSE72094: 386 LUAD patients, GSE36471: 112 LUAD patients) with a follow-up period longer than 30 days were screened out for further validation. Among the four external validations, tumor relapse annotation and disease-free survival time were well documented in GSE30219. Additionally, mRNA expression data of 42 melanoma patients treated with immune checkpoint inhibitors (ICIs) and 25 melanoma patients treated with adoptive T cell therapy (ACT) were selected for the prediction of the response to immunotherapy. All of the raw CEL files collected from the GEO database were processed using the Robust Multichip Average (RMA) algorithm for background adjustment and quantile normalization. Details of the datasets used in this study are presented in Table 1.

### 2.2 | Differential expression analysis

In this part, R package “survminer” (Available from: <https://CRAN.R-project.org/package=survminer>) was used to identify the best cut-off points for estimating survival in mRNasi and immune score and draw survival curves.<sup>15</sup> Based on the optimal survival tipping point of

TABLE 1 Data sets used in this study

| Data sets  | Source    | PMID     | Sample size for each group | Platform/Technology                                       |
|--|-----------|----------|----------------------------|---|
| Discovery set ( $n = 484$ )                        | TCGA-LUAD | \        |                            | Illumina HiSeq  |
| External testing set ( $n = 309$ )                 | GSE31210  | 23028479 | 226                        | Affymetrix Human Genome U133 Plus 2.0 Array               |
|  | GSE30219  | 23698379 | 83                         | Affymetrix Human Genome U133 Plus 2.0 Array               |
| External validation set ( $n = 498$ )              | GSE36471  | 22590557 | 112                        | Agilent-UNC-custom-4X44K                                  |
|  | GSE72094  | 26477306 | 386                        | Rosetta/Merck Human RSTA Custom Affymetrix 2.0 microarray |
| Immunotherapy response validation set ( $n = 67$ ) | TCGA-SKCM | 30842092 | 42                         | Illumina HiSeq  |
|  | GSE100797 | 29170503 | 25                         | Illumina HiSeq  |
| Radiotherapy response validation set ( $n = 49$ )  | TCGA-LUAD | \        | 49                         | Illumina HiSeq  |
| Relapse response validation set ( $n = 83$ )       | GSE30219  | 23698379 | 83                         | Affymetrix Human Genome U133 Plus 2.0 Array               |

mRNasi and immune score, 484 patients with lung adenocarcinoma were divided into the high/low-mRNasi group and high/low-immune score group. Kaplan–Meier curves for overall survival (OS) were analyzed using the R package “survival”. The differentially expressed genes (DEGs) between the high-mRNasi-low-immune score group and other groups were generated by R package “limma” based on  $|\text{LogFC}| > 1$  and  $\text{FDR} < 0.05$ . The upregulated genes and down-regulated genes in the high-mRNasi-low-immune score group were regarded as TSI-related genes.

### 2.3 | Construction of TSISig

A total of 484 LUAD patients from TCGA were randomly divided into training ( $n = 242$ ) and test ( $n = 242$ ) groups. Univariate Cox regression analysis was used to analyze the association between DEGs and overall survival time to screen out prognostic tumor stemness and immune infiltration (TSI)-related genes ( $p < 0.05$ ). Least absolute shrinkage and selection operator (LASSO), which could generate a penalty function to compress the variable coefficients in the regression model to prevent over fitting, was performed to further select prognostic TSI-related genes. After multivariate COX regression analysis, expression values of the selected TSI-related genes weighted by the multivariate Cox regression coefficient were subsequently converted to a risk score and TSISig was successfully constructed. Then, Kaplan–Meier curves for overall survival analysis of TSISig were illustrated using the “survival” R

package. R package “survivalROC” was performed to generate a time-dependent receiver operating characteristic (ROC) curve.

### 2.4 | Gene set enrichment analysis (GSEA) and tumor immune dysfunction and exclusion (TIDE)

To explore the potential function of TSISig, GSEA software was used for enrichment analysis of the biological process (BP) and Kyoto Encyclopedia of Genes and Genomes (KEGG). TIDE is a newly developed computational method that can model the mechanisms of tumor immune evasion and predict the clinical response of patients to ICIs (<http://tide.dfci.harvard.edu/>)(30127393,32102694). In this study, we calculated the TIDE score of 484 LUAD patients from TCGA and predicted the clinical response of these patients to ICIs.

### 2.5 | Evaluation of TMB with TSISig in TCGA-LUAD

Somatic variants with the Mutation Annotation Format (MAF) for LUAD patients were obtained from the TCGA database. R package “maftools” was used for visualization. The TMB value was calculated as (mutation frequency with a number of variants)/the length of exons (38 million).<sup>16</sup> According to the median TMB, patients

with LUAD were further divided into high-TMB and low-TMB groups.

## 2.6 | Identification of potential compounds targeting TSISig

The connectivity map (CMap) is an online drug genome database<sup>17</sup> that allows researchers to explore the potential relationship between genes and compounds. To screen the underlying candidate compounds targeting TSISig, we analyzed the DEGs between high risk and low risk using the R package “limma” and selected the top 150 up-regulated genes and 150 down-regulated genes as genes co-expressed with TSISig to query the database. Compounds with enrichment scores  $\leq 97$  were regarded as effective inhibitors that could target TSISig.

## 2.7 | Statistical analysis

The Wilcoxon rank-sum test was used to compare 2 groups, and the Chi-square test was performed for comparisons of more than 2 groups. Survival curves for each data set were illustrated using the Kaplan–Meier method. Univariate Cox regression analysis was applied to calculate the hazard ratios of indexes, and multivariate Cox regression analysis was used to measure independent prognostic factors. The Spearman method was used to calculate the correlation coefficients. All statistical analyses were performed using R (version: 4.0.3).  $p < 0.05$  was considered significant.

# 3 | RESULTS

## 3.1 | Identification of specific genes related to tumor stemness and immune infiltration

In this part, the aim of our study was to screen out TSI-related genes for LUAD patients. Spearman analysis showed that mRNAsi was significantly negatively correlated with the immune score of 484 LUAD patients from TCGA (Figure 1A). After performing R package “survminer,” the best cut-off points for estimating OS in mRNAsi and the immune score were identified respectively as 0.36 and 1798.36 (Figure S2A,B). According to the best cut-off points for estimating survival, 484 LUAD patients from TCGA were divided into high/low-mRNAsi groups and high/low-immune score groups (Figure 1B,C). Then, four combinatorial groups were generated: high-mRNAsi-low-immune score

group, high-mRNAsi-high-immune score group, low-mRNAsi-low-immune score group, and low-mRNAsi-high-immune score group. Kaplan–Meier curves for overall survival among the four combinatorial groups suggested that these four subgroups had significant differences in OS ( $p = 0.0026$ ) (Figure 1D), and the prognosis of the high-mRNAsi-low-immune score group was worse than that of the other groups ( $p = 0.0025$ ) (Figure 1E). Comparisons of clinical characteristics (including gender, age, TNM stage, radiotherapy, race, and TMB) showed that gender, age, stage, T stage, and TMB were significantly different between the high-mRNAsi-low-immune score group and others (Chi-square test: gender,  $p = 0.027$ ; age,  $p = 0.046$ ; stage,  $p = 0.025$ ; T stage,  $p = 0.04$ ; TMB,  $p < 0.001$ ) (Table 2). In order to explore the underlying mechanism in the poor OS groups, 94 upregulated genes and 286 down-regulated genes in the high-mRNAsi-low-immune score group were identified using R package “limma” ( $|\text{LogFC}| > 1$  and  $\text{FDR} < 0.05$ ) (Figure 1F, Figure S2C). These genes were regarded as tumor stemness and immune infiltration (TSI)-related genes.

## 3.2 | Construction and validation of TSISig

After univariate Cox regression analysis for the 300 TSI-specific genes, 155 genes ( $p < 0.05$ ) were selected for LASSO Cox regression analysis (Figure 2A). Five TSI-specific genes (CPS1, CCR2, NT5E, ANLN, and ABCC2) were screened out by multivariate Cox regression analysis for the construction of TSISig based on the TCGA-training set (C-index: 0.73) (Figure 2B). All the five TSI-specific genes were independent risk factors for OS in the training and test set. To facilitate clinical application, we calculated the TSISig risk score of samples using the following formula:  $\text{risk score} = (-1.5502) \times (\text{expression level of CCR2}) + 0.748 \times (\text{expression level of CPS1}) + 1.7482 \times (\text{expression level of NT5E}) + 1.5344 \times (\text{expression level of ANLN}) + 1.1436 \times (\text{expression level of ABCC2})$ . All patients in the training set ( $n = 242$ ) were divided into high ( $n = 121$ ) and low-risk ( $n = 121$ ) groups according to the median TSISig risk score (0.893). The OS survival analysis indicated that patients in the low-risk group had a better prognosis ( $p < 0.0001$ ) (Figure 2C). The time-dependent ROC analysis showed that the area under the curve (AUC) of TSISig was 0.856 and 0.756 at 1- and 2-year OS respectively (Figure 2D). In addition, univariate and multivariate Cox regression analyses for clinical factors and TSISig indicated that TSISig (HR:1.479,  $p < 0.001$ ) and stage (HR: 1.503,  $p < 0.001$ ) were independent predictors of LUAD (Figure 2E).

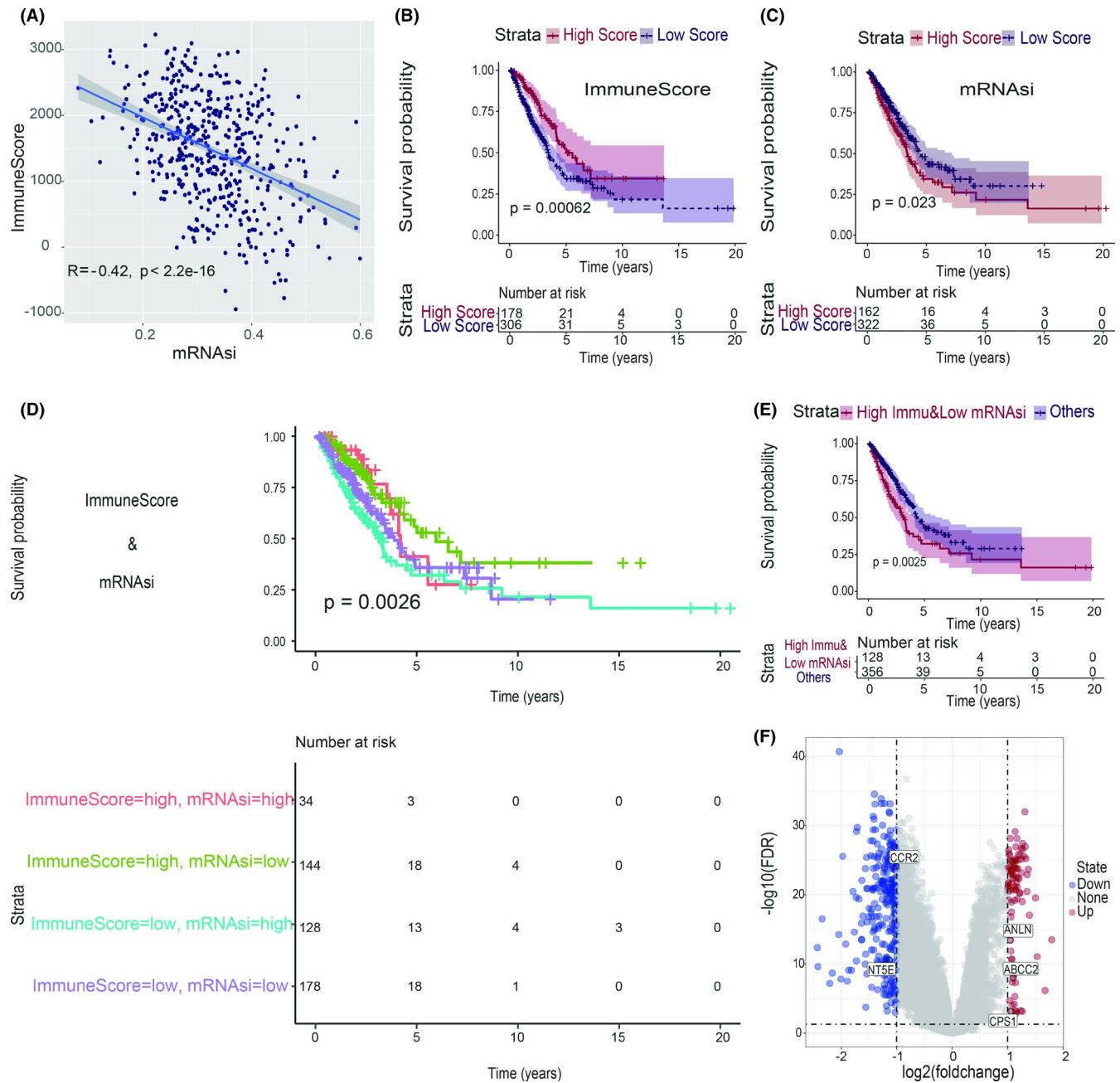


**FIGURE 1** Identification of TSI-specific genes. (A) Correlation between mRNA<sub>si</sub> and immune score in LUAD based on TCGA database. (B-C) Kaplan-Meier curves for overall survival in patients with LUAD based on the optimal survival tipping points of immune score or mRNA<sub>si</sub>. (D-E) Kaplan-Meier curves for overall survival among four combination groups. (F) Identification of DEGs between high-mRNA<sub>si</sub>-low-immune score group and others ( $|\log_{2}FC| > 1$  and  $FDR < 0.05$ ).

To validate the predictive ability of TSI<sub>sig</sub>, we calculated the TSI<sub>sig</sub> risk score of LUAD patients in the TCGA testing set ( $n = 242$ ), external testing set ( $n = 309$ ), and external validation set ( $n = 498$ ). Patients were then divided into high- and low-risk groups with an optimal cut-off value (0.893) obtained from training set analysis. The OS analysis for the testing and validation sets showed that patients with LUAD in the low-risk group had a better prognosis than those in the high-risk group ( $p < 0.05$ ).

Time-dependent ROC analysis was then performed to assess the prognostic accuracy of TSI<sub>sig</sub>, and the AUCs for 1- and 2-year OS were all over 0.7 for the testing and validation sets. Univariate and multivariate Cox regression analyses in the testing and validation sets demonstrated that TSI<sub>sig</sub> and stage were independent prognostic factors for LUAD patients (Figure 3A-C, Figure S3A-G). These results suggested that TSI<sub>sig</sub> had a good predictive ability for the OS of patients with LUAD.

TABLE 2 Patient characteristics (bold values means that  $p$  value is  $<0.05$ )

| Variable         | Low immunescore & High mRNAsi ( $n = 128$ ) | Others ( $n = 356$ ) | Total ( $n = 484$ ) | X-squared | $p$ -value       |
|------------------|---|----------------------|---------------------|-----------|------------------|
| Gender           |   |                      |                     | 4.9143    | <b>0.027</b>     |
| Female           | 57  | 201                  | 258                 |           |                  |
| Male             | 71  | 155                  | 226                 |           |                  |
| Age              |   |                      |                     | 6.1678    | <b>0.046</b>     |
| <65 years        | 68  | 144                  | 212                 |           |                  |
| $\geq 65$ years  | 58  | 204                  | 262                 |           |                  |
| Unknown          | 2   | 8                    | 10                  |           |                  |
| Stage            |   |                      |                     | 11.154    | <b>0.025</b>     |
| I                | 53  | 206                  | 259                 |           |                  |
| II               | 37  | 77                   | 114                 |           |                  |
| III              | 26  | 52                   | 78                  |           |                  |
| IV               | 10  | 15                   | 25                  |           |                  |
| Unknown          | 2   | 6                    | 8                   |           |                  |
| T                |   |                      |                     | 9.3981    | <b>0.04</b>      |
| T1               | 31  | 130                  | 161                 |           |                  |
| T2               | 73  | 187                  | 260                 |           |                  |
| T3               | 17  | 25                   | 42                  |           |                  |
| T4               | 6   | 12                   | 18                  |           |                  |
| Unknown          | 1   | 2                    | 3                   |           |                  |
| N                |   |                      |                     | 7.6201    | 0.11             |
| N0               | 74  | 239                  | 313                 |           |                  |
| N1               | 29  | 63                   | 92                  |           |                  |
| N2               | 24  | 43                   | 67                  |           |                  |
| N3               | 0   | 2                    | 2                   |           |                  |
| Unknown          | 1   | 9                    | 10                  |           |                  |
| M                |   |                      |                     | 4.0332    | 0.13             |
| M0               | 86  | 232                  | 318                 |           |                  |
| M1               | 10  | 14                   | 24                  |           |                  |
| Unknown          | 32  | 110                  | 142                 |           |                  |
| RT               |   |                      |                     | 3.3163    | 0.19             |
| Yes              | 19  | 38                   | 57                  |           |                  |
| No               | 85  | 266                  | 351                 |           |                  |
| Unknown          | 24  | 52                   | 76                  |           |                  |
| Race             |   |                      | 0                   | 3.8963    | 0.27             |
| African American | 19  | 34                   | 53                  |           |                  |
| White            | 92  | 279                  | 371                 |           |                  |
| Asian            | 3   | 4                    | 7                   |           |                  |
| Unknown          | 14  | 39                   | 53                  |           |                  |
| TMB              |   |                      |                     | 28.665    | <b>&lt;0.001</b> |
| High             | 88  | 149                  | 237                 |           |                  |
| Low              | 37  | 201                  | 238                 |           |                  |
| Unknown          | 3   | 6                    | 9                   |           |                  |

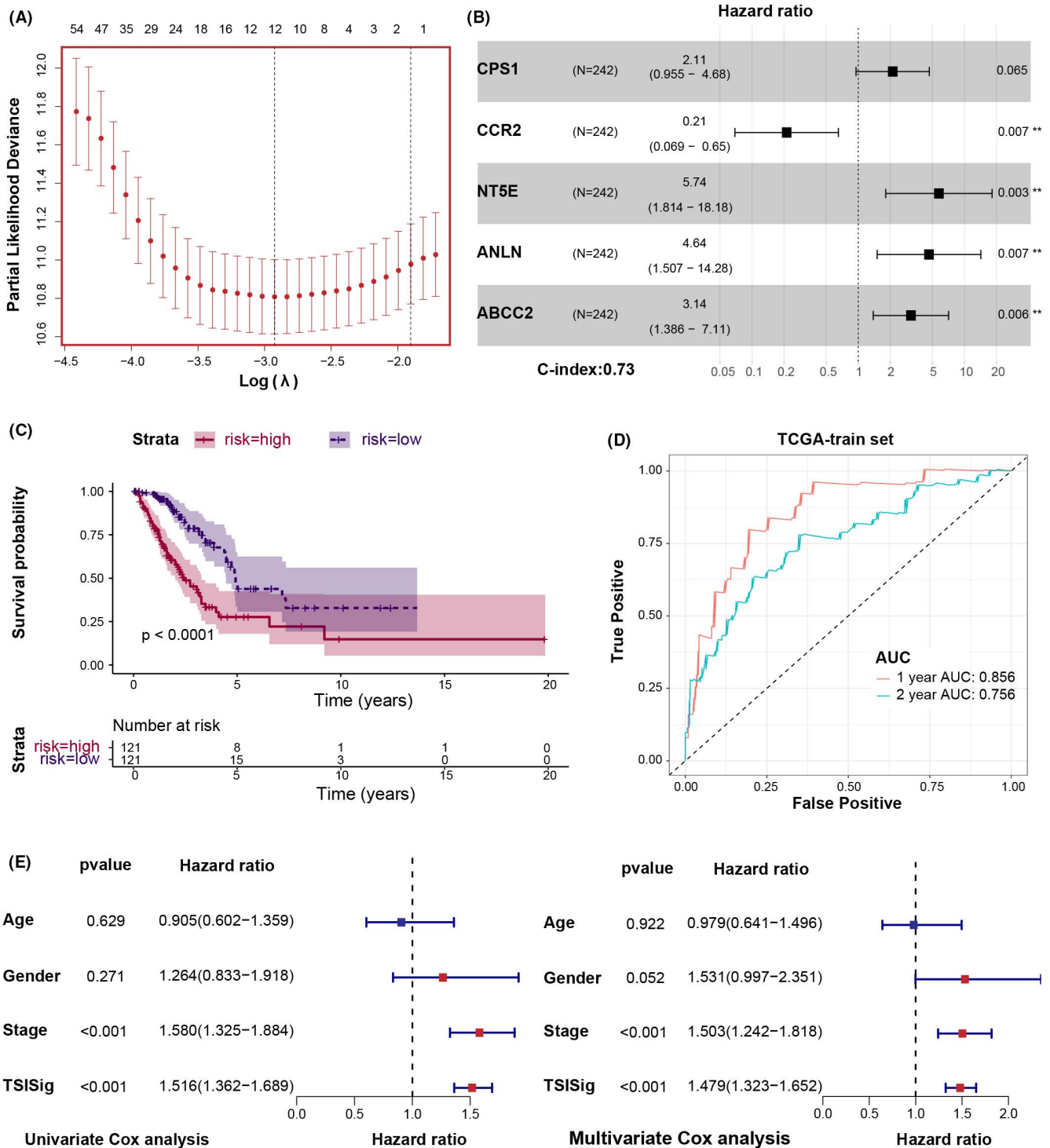


**FIGURE 2** Construction of TSISig based on TCGA training set. (A) LASSO Cox regression analysis for TSI-specific genes. (B) Multivariate Cox analysis for the five TSI-specific genes contained in TSISig. (C) Overall survival analysis for the low and high TSISig groups. (D) Time-dependent ROC curve for prediction of prognosis in the training set. (E) Forest plot for the HRs of TSISig and clinicopathological factors calculated by univariate Cox and multivariate Cox analysis.

### 3.3 | Function validation of TSISig

To validate whether TSISig could coordinate tumor stemness and immune infiltration, 484 LUAD patients from TCGA were ranked based on mRNasi (Figure 4A)

and immune score (Figure 4B). Compared to the high-risk group, the low-risk group had lower mRNasi and higher immune score (Figure 4C). Then, 10 immune subpopulations of 484 LUAD tissues from TCGA were estimated using the MCP counter. Enrichment analysis

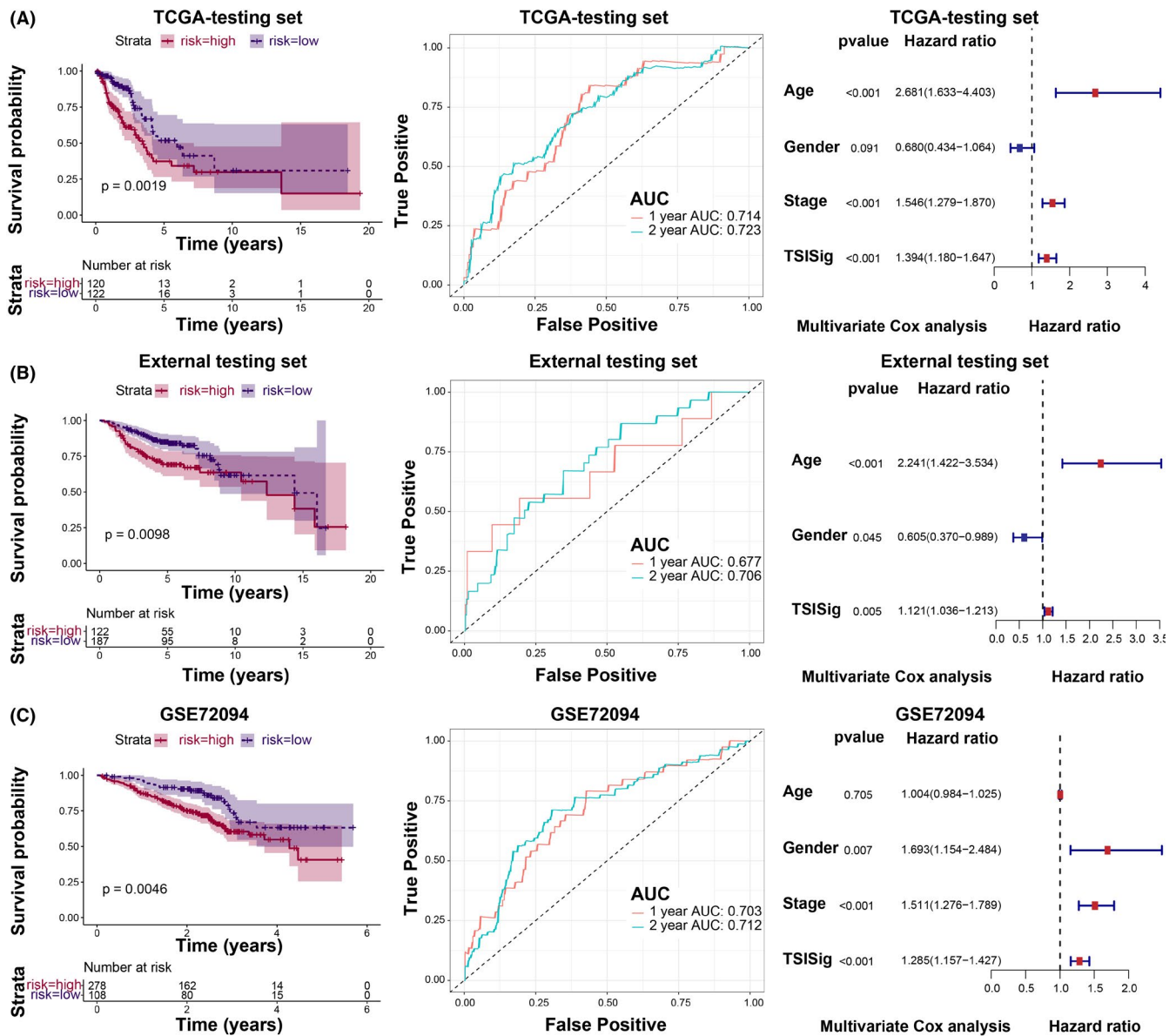


**FIGURE 3** Validation of TSISig in TCGA testing set, external testing set, and GSE72094. (A) Overall survival analysis, time-dependent ROC curve, and multivariate Cox analysis in TCGA testing set. (B) Overall survival analysis, time-dependent ROC curve, and multivariate Cox analysis in external testing set. (C) Overall survival analysis, time-dependent ROC curve, and multivariate Cox analysis in GSE72094.

of the immune subpopulations indicated that myeloid dendritic cells, B lineage, T cells, endothelial cells, monocytic lineage, CD8 T cells, cytotoxic lymphocytes, and neutrophils were highly enriched in the low-risk group, and fibroblasts and NK cells were mainly enriched in the high group (Figure 4D). GSEA showed that the high-risk group was highly associated with the cell cycle, DNA replication, P53 signaling pathway, and regulation of cell aging, and the low-risk group was mainly enriched in cell adhesion molecules (CAMs), B cell receptor signaling pathway, T cell-mediated immunity, humoral immune response, immune response regulation signaling pathway, and activation of the immune response (Figure 4E). All these results suggested that

TSISig was significantly correlated with tumor stemness and immune infiltration.

### 3.4 | TSISig was associated with TMB

Considering the significant difference in TMB between the high-mRNAi-low-immune score group and the others, we tried to analyze the relationship between TSISig and TMB. In the waterfall map of the top 20 mutations, we found that the mutation frequency in the high-risk group was significantly higher than that in the low-risk group (Figure 5A). The box plot showed that the high-risk group had a higher TMB than the

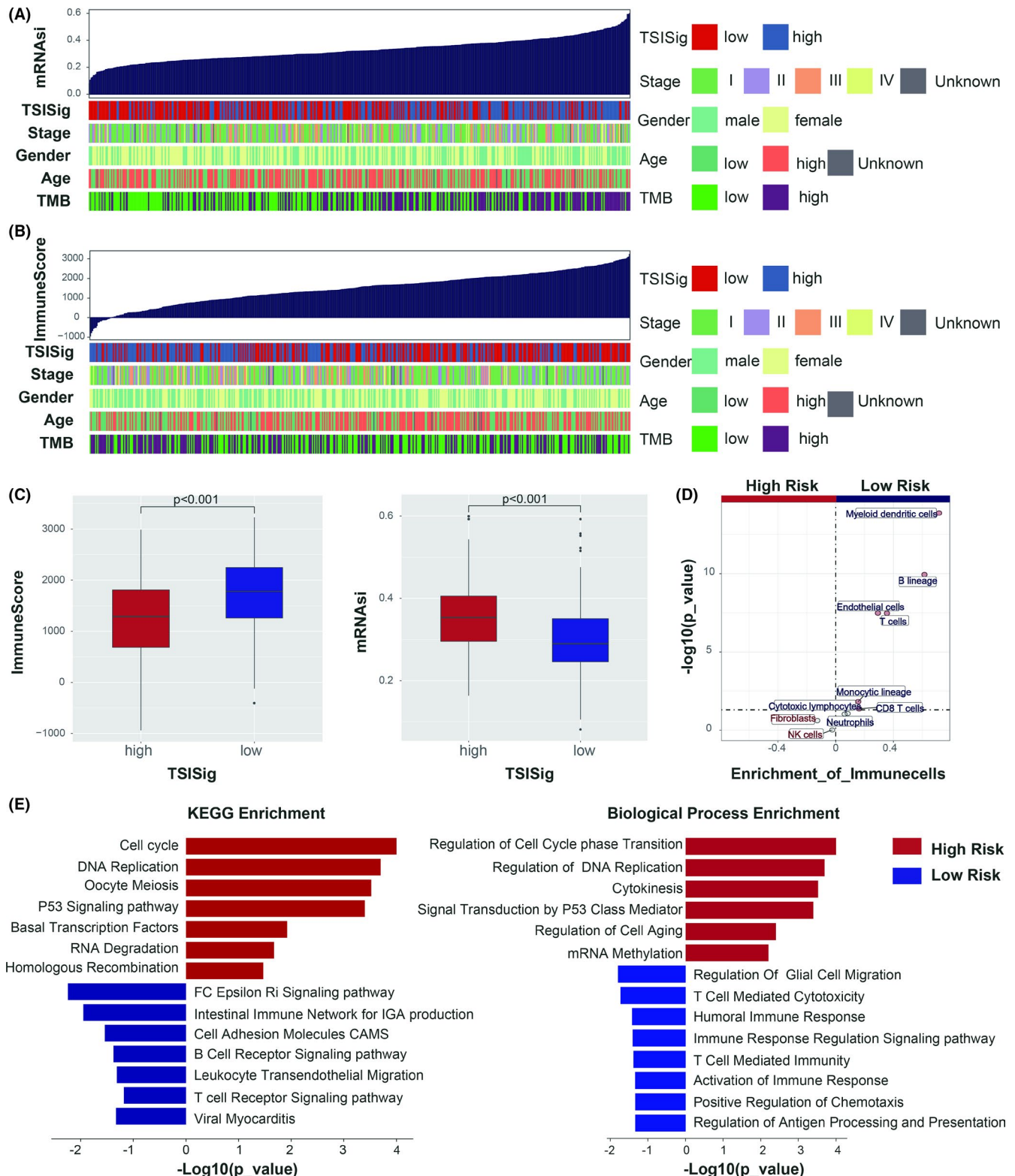


**FIGURE 4** Function characterization of TSISig. (A-B) A general description of the association between mRNAasi or immune score and TSISig or clinicopathological factors. (C) Box plots for the distribution of mRNAasi/immune score in low and high TSISig. (D) Enrichment of immune subpopulations in low and high TSISig. (E) KEGG pathways and biological process enrichment analysis using GSEA.

low-risk group ( $p < 0.001$ ) (Figure 5B). Chisp-test analysis for the top 20 gene mutations showed that TP53, TTN, RYR2, CSMD3, LRP1B, ZFH4, USH2A, SPTA1,

FLG, NAV3, and FAT3 had higher mutation rates in the high-risk group (Table S1). OS analysis suggested that patients with high TSISig and low TMB had the worst

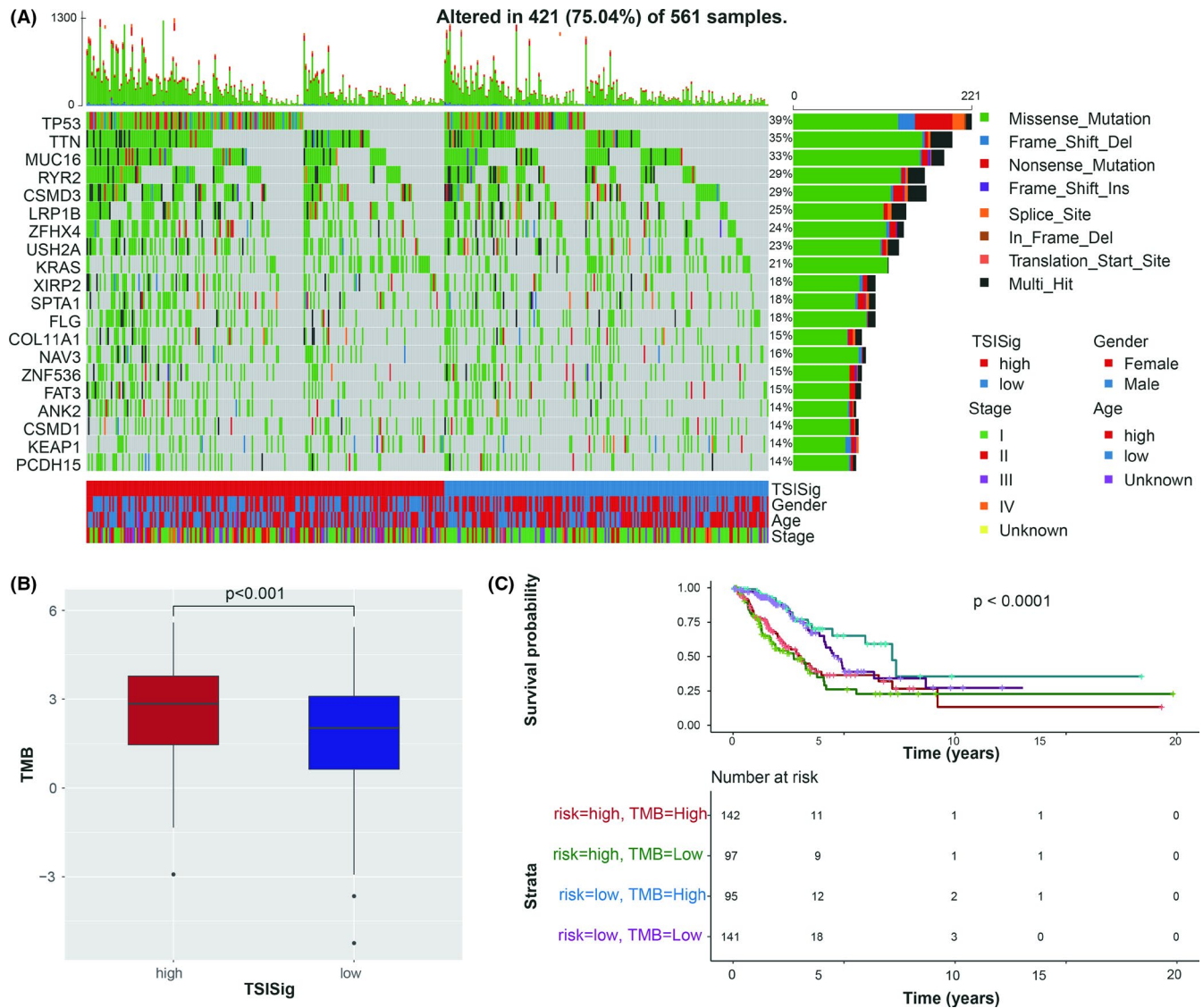
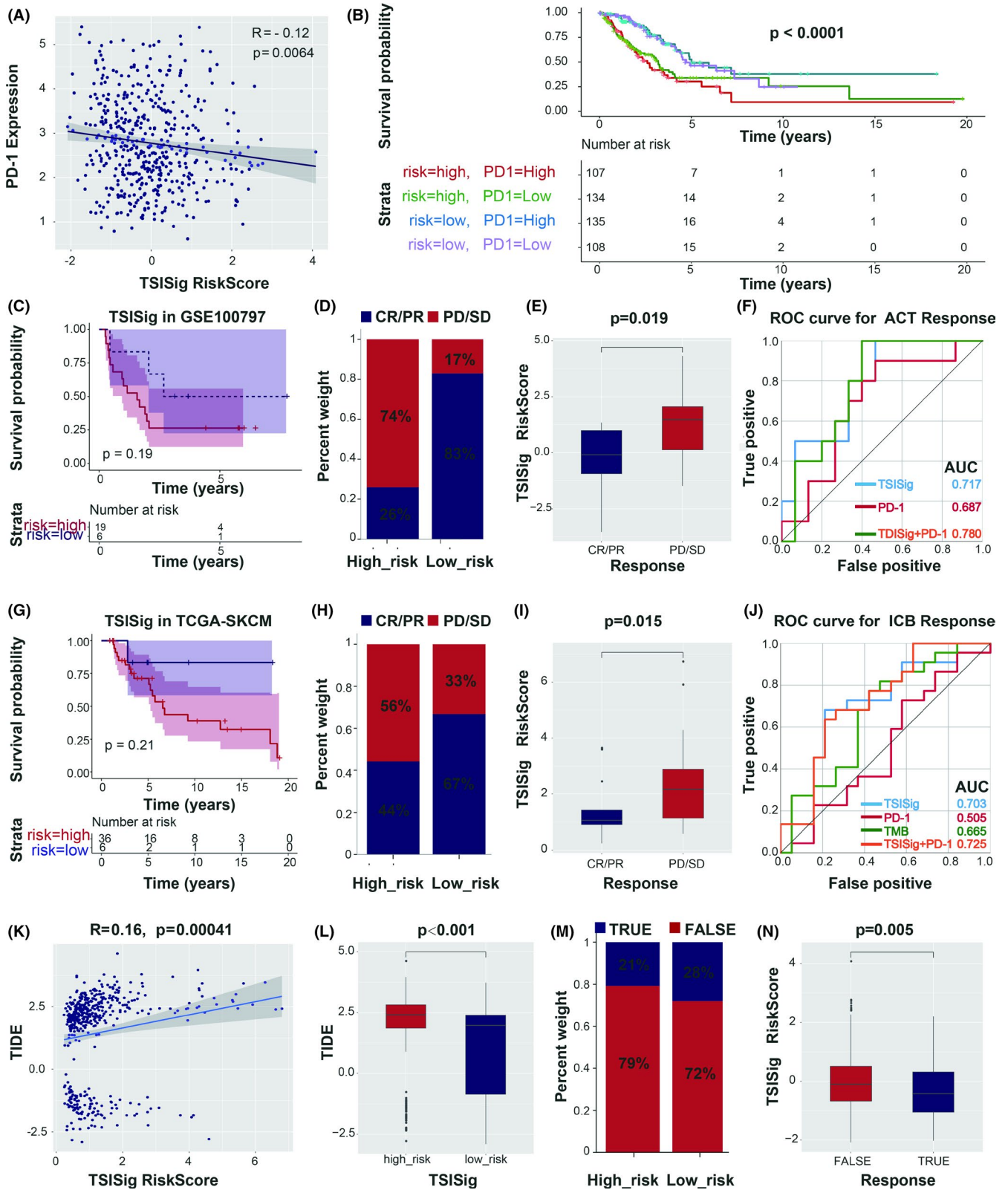


**FIGURE 5** Correlation between cancer somatic genome and TSI Sig. (A) Distribution of top 20 highly variant mutated genes in low and high TSI Sig. (B) Difference of tumor mutation burden (TMB) between low and high TSI Sig. (C) Kaplan–Meier curves for four combination groups classified by TSI Sig and TMB.

prognosis, while patients with low TSI Sig and high TMB had the best prognosis ( $p < 0.0001$ ) (Figure 5C). In summary, there was a positive correlation between

TSI Sig and TMB, and the combined detection of TSI Sig and TMB might better predict the prognosis of patients with LUAD.

**FIGURE 6** Estimation of predictive ability for TSI Sig to immunotherapy response. (A) Association between PD-1 expression and TSI Sig. (B) Overall survival analysis for four combination groups stratified by PD-1 and TSI Sig. (C) Kaplan–Meier curves for patients with low and high TSI Sig in GSE100797. (D) Clinical response rate of patients with low and high TSI Sig for adoptive T cell therapy (ACT) in GSE100797 (complete response [CR], partial response [PR], stable disease [SD], progressive disease [PD]). (E) Difference of TSI Sig risk score in different ACT response (Wilcoxon rank-sum test,  $p = 0.019$ ). (F) ROC curves estimating the predictive value of TSI Sig, PD-1 expression, and the combination of TSI Sig and PD-1 in GSE100797. (G) Kaplan–Meier curves for patients with low and high TSI Sig in TCGA-SKCM patients with ICIs treatment. (H) Clinical response rate of patients with low and high TSI Sig for ICIs in TCGA-SKCM data set. (I) Difference of TSI Sig risk score in different ICIs therapy response (Wilcoxon rank-sum test,  $p = 0.015$ ). (J) ROC curves estimating the predictive value of TSI Sig, PD-1 expression, TMB, and the combination of TSI Sig and PD-1 in TCGA-SKCM patients with ICIs treatment. (K) Correlation between tumor immune dysfunction and exclusion (TIDE) score and TSI Sig in TCGA-LUAD. (L) Distribution of TIDE score in low and high TSI Sig (Wilcoxon rank-sum test,  $p < 0.001$ ). (M) Clinical response rate of patients with low and high TSI Sig for ICIs therapy in TCGA-LUAD. (N) Difference of TSI Sig risk score in different ICIs therapy response predicted by TIDE (Wilcoxon rank-sum test,  $p = 0.005$ ).



### 3.5 | Predictive ability of TSISig of immunotherapeutic benefits

Emerging evidence has suggested that monoclonal antibodies against PD1 immune checkpoints could inhibit the development of cancers and prolong the patient's OS.<sup>18</sup>

After examining the correlation between PD-1 expression and TSISig risk score in TCGA-LUAD patients, we found that there was a significant negative correlation between TSISig and PD-1 expression (Figure 6A). Then, 484 LUAD patients from TCGA were classified into high-PD-1 expression and low-PD-1 expression groups according to

the median expression of PD-1. Kaplan–Meier curves for OS showed that high-PD-1 expression and low-TSISig group had the best prognosis compared to the other three groups (Figure 6B). These results led us to believe that TSISig might be able to predict the response of LUAD patients to immunotherapy. At present, the study of tumor-associated antigen in melanoma is the most successful. Compared with other cancers, melanoma is a tumor with stronger immunogenicity and better responses to immunotherapy.<sup>19</sup> Therefore, the majority of the current immunotherapy studies aimed at melanoma. We searched the GEO and TCGA databases and found no suitable immunotherapeutic LUAD expression data. Considering the lack of public data on immunotherapy for lung cancer, two melanoma datasets treated with immune checkpoint inhibitors or ACT were downloaded to examine the predictive ability of TSISig. According to TSISig, we calculated the risk score of patients in TCGA-SKCM (treated with ICIs,  $n = 42$ ) and GSE100797 (treated with ACT,  $n = 25$ ). Survival analysis indicated that the low-risk group had a better prognosis than the high-risk group in both TCGA-SKCM and GSE100797 (Figure 6C,G). However, we did not obtain meaningful results (GSE100797,  $p = 0.19$ ; TCGA-SKCM,  $p = 0.21$ ), which might have been due to the small sample size. Moreover, in both cohorts, the proportion of CR/PR patients in the high-risk group was significantly lower than that in the low-risk group (GSE100797: high-risk group: CR/PR: 26%, PD/SD: 74%; low-risk group: CR/PR: 83%, PD/SD: 17%; TCGA-SKCM: high-risk group: CR/PR: 44%, PD/SD: 56%; low-risk group: CR/PR: 67%, PD/SD: 33%) and PD/SD patients had higher TSISig risk scores than CR/PR patients (GSE100797,  $p = 0.019$ ; TCGA-SKCM,  $p = 0.015$ ) (Figure 6D,E,H,I). Furthermore, compared to using TSISig and PD-1 expression alone, the combined score was the best at predicting CR/PR in two cohorts (GSE100797, AUC: TSISig: 0.717, PD-1: 0.687, TSISig & PD-1: 0.780; TCGA-SKCM, AUC: TSISig: 0.703, PD-1: 0.505, TSISig & PD-1: 0.725). The predictive ability of TSISig for the response to immunotherapy was higher than that of TMB in TCGA-SKCM (AUC: TSISig: 0.703, TMB: 0.665) (Figure 6F,J). Additionally, we performed TIDE online tools to estimate the response and TIDE scores of 484 LUAD patients from TCGA to ICIs, and the results demonstrated that TSISig was significantly positively correlated with TIDE score ( $r = 0.16$ ,  $p = 0.00041$ ) (Figure 6K). Patients with high TSISig had higher TIDE scores than patients with low TSISig ( $p < 0.001$ ) (Figure 6L), and the proportion of patients with true response to ICIs in the high-TSISig group was also higher than that in the low-TSISig group (high TSISig: true: 21%, false: 79%; low TSISig: true, 28%; false, 72%) (Figure 6M). The box plot showed that the group with a true response to ICIs had lower TSISig scores ( $p = 0.005$ ) (Figure 6N). All these

results suggest that TSISig could serve as an excellent predictor of immunotherapeutic benefits.

### 3.6 | Predictive ability of TSISig for the response to radiotherapy and tumor relapse

Previous studies have revealed that radiotherapy and immune suppression might improve tumor stemness and lead to tumor relapse.<sup>20</sup> We attempted to investigate the predictive ability of TSISig for the response to radiotherapy and tumor relapse. Forty-nine patients with LUAD who received radiotherapy were selected for the prediction of their response to radiotherapy. Patients with low TSISig showed a better prognosis (OS,  $p = 0.05$ ) (Figure 7A) and a higher proportion of CR/PR response (high-risk group: CR/PR: 28%, PD/SD: 72%; low-risk group: CR/PR: 45%, PD/SD: 55%) (Figure 7B). Moreover, a higher TSISig risk score was observed in PD/SD patients ( $p = 0.025$ ) (Figure 7C), and the ROC curve showed a good ability of TSISig to predict the response to RT (AUC: 0.691) (Figure 7D). Furthermore, we found that patients with low TSISig in GSE30219 had a longer disease-free survival (DFS,  $p = 0.082$ ) (Figure 7E) and lower tumor recurrence rate than patients with high TSISig (high-risk group: relapse, 44%; no-relapse, 56%; low-risk group, relapse: 25%, no-relapse: 75%) (Figure 7F). In addition, our results demonstrated that tumor relapse patients had higher TSISig risk scores ( $p = 0.047$ ) (Figure 7G), and TSISig could partly predict tumor recurrence (AUC = 0.636) (Figure 7H).

### 3.7 | Mining underlying compounds or inhibitors targeting TSISig based on CMap

The top 150 upregulated genes and 150 downregulated genes in high TSISig were selected to query the CMap database. Compounds or inhibitors with an enrichment score  $\leq -97$  were considered effective inhibitors targeting TSISig. Only the compounds that were treated with A549 cells (lung cancer cells) were selected. Finally, 65 compounds or inhibitors and related 48 mechanisms of action from the mode-of-action (MoA) analysis were screened out (Figure 8, Table S2). The top hits showed that 9 inhibitors (THM-I-94, apicidin, NSC-3852, vorinostat, HC-toxin, panobinostat, trichostatin-a, ISOX, and dacinostat) shared the MoA of HDAC inhibition, and 8 inhibitors (doxorubicin, etoposide, irinotecan, camptothecin, mitoxantrone, teniposide, pirarubicin, amonafide) shared the MoA of topoisomerase inhibition. In addition, PHA-793887 and JNJ-7706621 shared the MoA of CDK inhibition, and manumycin-a and CAY-10470 shared the MoA of NFkB

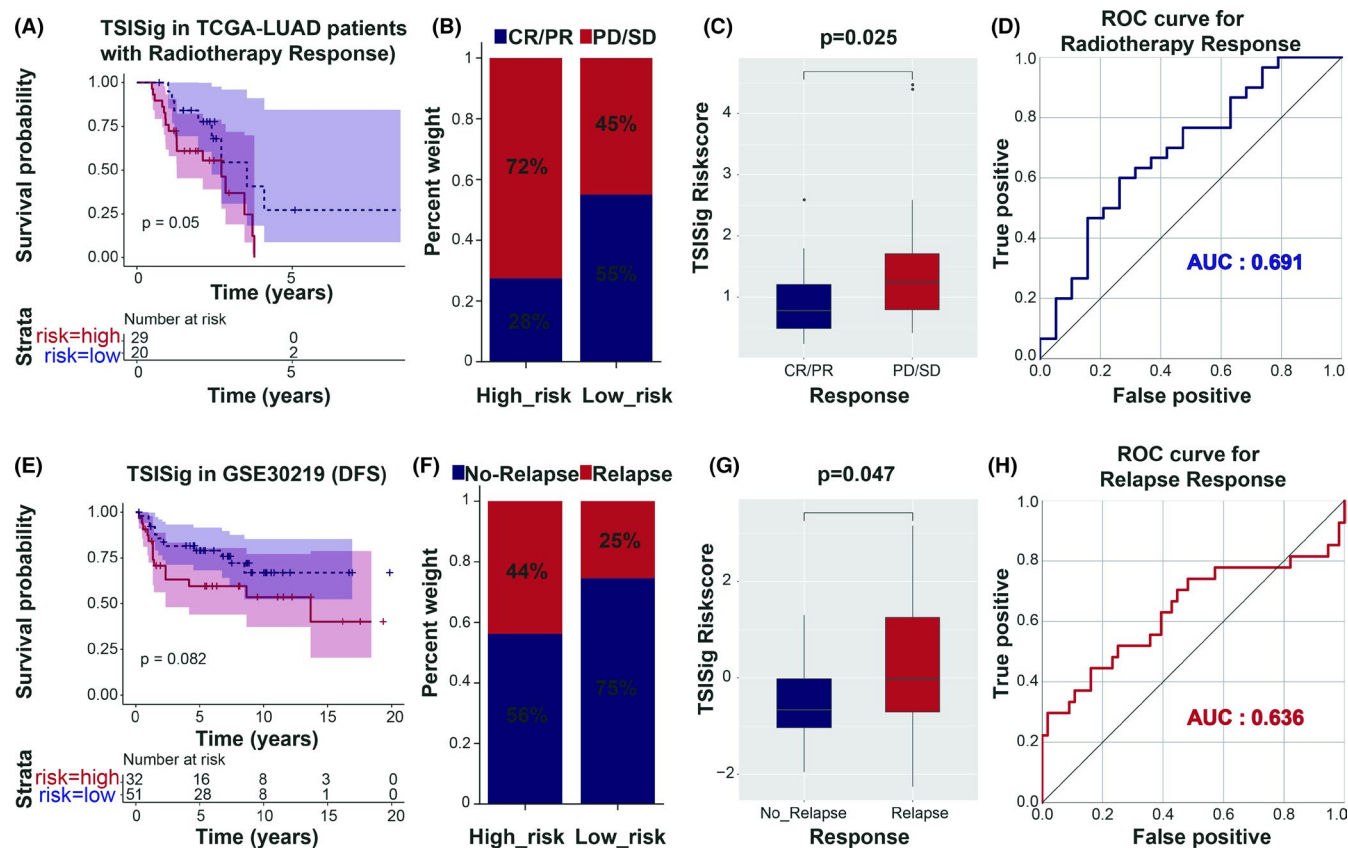


**FIGURE 7** Assessment of predictive ability for TSISig to radiotherapy and tumor recurrence. (A) Kaplan–Meier curves for patients with low and high TSISig in TCGA-LUAD patients with radiotherapy. (B) Clinical response rate of patients with low and high TSISig for radiotherapy in TCGA-LUAD patients with radiotherapy (complete response [CR], partial response [PR], stable disease [SD], progressive disease [PD]). (C) Difference of TSISig risk score in different radiotherapy response (Wilcoxon rank-sum test,  $p = 0.025$ ). (D) ROC curves estimating the predictive value of TSISig to radiotherapy in TCGA-LUAD patients with radiotherapy. (E) Kaplan–Meier curves for disease free survival (DFS) in patients with low and high TSISig in GSE30219. (F) Tumor relapse rate of patients with low and high TSISig in GSE30219. (G) Difference of TSISig risk score between relapse and no-relapse LUAD patients (Wilcoxon rank-sum test,  $p = 0.047$ ). (H) ROC curves estimating the predictive value of TSISig to tumor recurrence in GSE30219.

pathway inhibition. Two compounds (PI-103 and everolimus) were mTOR inhibitors.

## 4 | DISCUSSION

CSCs were defined as a subgroup of tumor cells that could initiate and maintain tumor growth through the ability of self-renewal, differentiation, and proliferation.<sup>21–23</sup> Previous studies have suggested that CSCs contribute to the development, chemotherapy resistance, radiation resistance, and recurrence of various tumors such as NSCLC,<sup>24,25</sup> breast cancer,<sup>26</sup> liver cancer,<sup>27</sup> and melanoma,<sup>28</sup> which might be related to increased mutation load, cancer/testis antigen expression, and intratumoral heterogeneity in cancers with high stemness.<sup>29</sup> Although some studies have indicated that a higher tumor mutation load could prolong the OS of tumor patients by enhancing immune infiltration,<sup>30</sup> a significant negative association

between cancer stemness and anticancer immunity was observed.<sup>13,29</sup> Therefore, we believe that there might be a relationship between tumor stemness and immunosuppression. Lengerke et al. and Giacotti et al. suggested that there existed a class of specific genes that could regulate cancer development by coordinating tumor stemness maintenance and immune suppression,<sup>8,9</sup> which was consistent with our hypothesis. In this study, we attempted to comprehensively understand the underlying relationship and related mechanisms between tumor stemness and immune infiltration in LUAD by exploring the tumor stemness and immune infiltration (TSI)-specific genes.

mRNasi was calculated to present the tumor stemness index, and the immune score was used to estimate the immune infiltration level of each LUAD patient. The correlation analysis between mRNasi and immune score revealed that tumor stemness was highly negatively correlated with immune infiltration ( $R = -0.42$ ,  $p < 0.0001$ ). After classifying patients with LUAD into

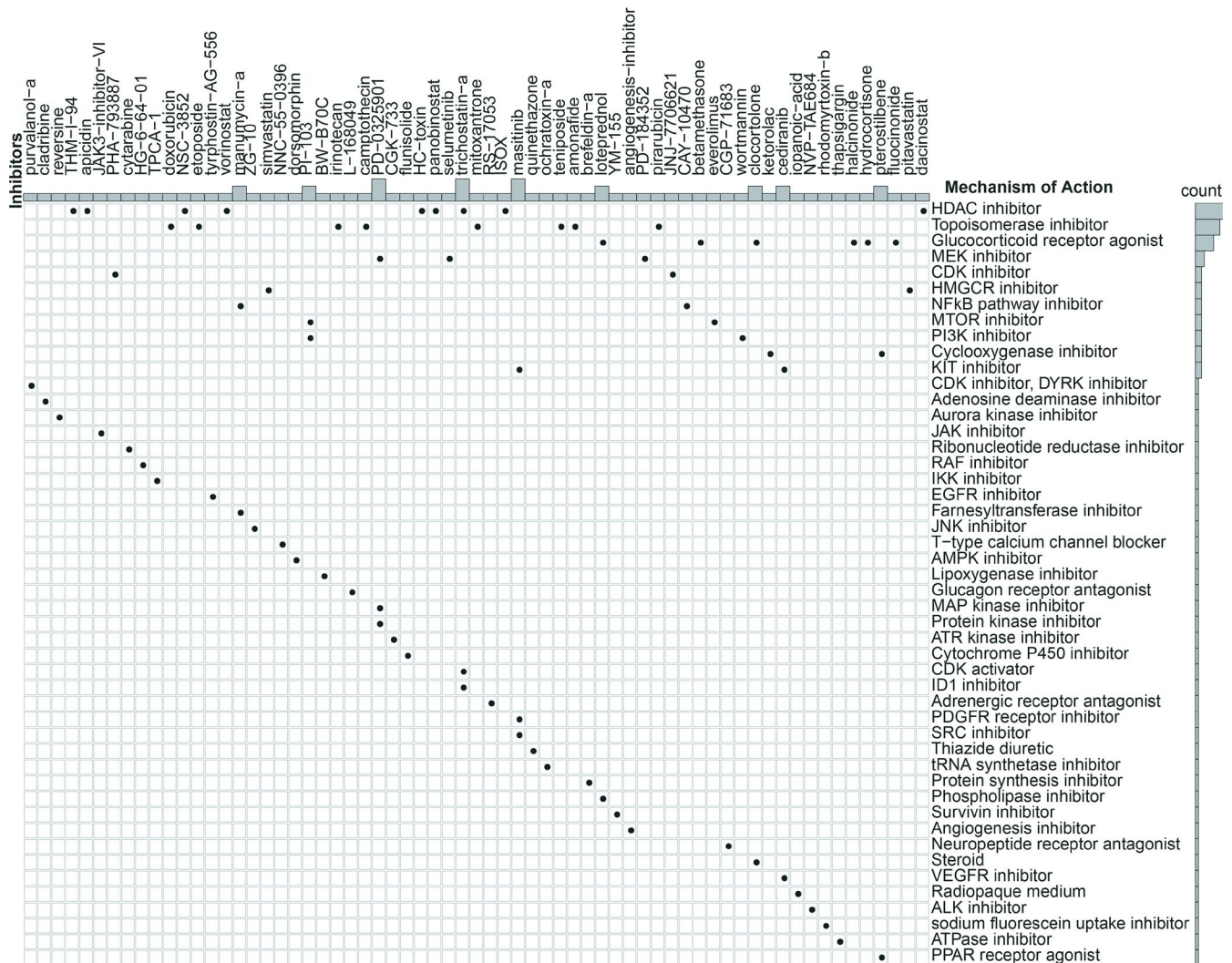


FIGURE 8 Heatmap exhibiting 65 compounds (enrichment score $\leq$ 97) and 48 related mechanisms of action (MOA, rows) which might target TSISig. Only the compounds that treated A549 cells (lung cancer cell) were selected.

high/low-mRNasi and high/low-immune score groups according to the optimal survival tipping point, four combinations were generated. Survival analysis showed that the high-mRNasi-low-immune score group had the worst OS ( $p < 0.01$ ). Clinical characteristic analysis indicated that male patients and patients aged  $\leq 65$  years might have a higher tumor stemness index and lower immune infiltration level. Advanced stage patients were inclined to have a higher tumor stemness index and lower immune infiltration level, which meant that these patients might have stronger immune suppression and tumor heterogeneity. Then, 380 DEGs between the high-mRNasi-low-immune score group and others were screened out as TSI-specific genes ( $|\text{LogFC}| > 1$  and  $\text{FDR} < 0.05$ ). Finally, a five-gene signature based on TSI-specific genes was constructed. Survival and ROC curve analysis in the training group, external testing, and external validation sets proved that TSISig had a good predictive ability for clinical prognosis. Moreover, univariate

and multivariate Cox analyses showed that TSISig and stage were independent prognostic indexes in LUAD. Compared with some models, our model has better prediction ability. A ten immune-related genes signature constructed by Jiaona Zhu et al.<sup>31</sup> and IPSLUAD signature established by Jie He<sup>32</sup> were believed to predict the prognosis of patients well. Compared with their signatures, TSISig had a higher AUC value in terms of predicting prognosis which indicated TSISig might have a better predictive ability. Although compared with the genes signature of Yongjian Zhang et al. TSISig had a lower AUC value,<sup>33</sup> TSISig was the first genes signature that could simultaneously predict the recurrence of LUAD and the efficacy of immunotherapy and radiotherapy. Further functional verification showed that TSISig was negatively correlated with immune score and positively correlated with mRNasi. Immune cell enrichment revealed that except for NK cells and fibroblasts, the other 8 kinds of immune cells, including CD8 T cells, cytotoxic

lymphocytes, and cells were mainly concentrated in the low-TSISig group and GSEA, suggesting that TSISig was mainly enriched in tumors and immune-related pathways. All these results were consistent with our previous work. Among the five TSI-specific genes, CPS1, NT5E, ANLN, and ABCC2 were correlated with poor prognosis, while CCR2 was correlated with better prognosis. CPS1, the urea cycle enzyme carbamoyl phosphate synthetase-1, could promote tumor growth by maintaining pyrimidine pools and DNA synthesis in KRAS/LKB1-mutant lung cancer cells.<sup>34</sup> NT5E (also known as CD73) was identified as an ecto-5'-nucleotidase that could induce antitumor immune responses and promote the proliferation, angiogenesis, and metastasis of cancers.<sup>35-37</sup> Some studies have regarded CD73 as a new immune checkpoint<sup>37</sup> and CD73 inhibitors are currently in the clinical trial stage of lung cancer.<sup>38</sup> ANLN encodes an actin-binding protein that is necessary for cytokinesis. Previous studies have suggested that ANLN plays an important role in cell growth and migration of breast cancer,<sup>39</sup> LUAD,<sup>40</sup> and pancreatic cancer.<sup>41</sup> ABCC2 from the superfamily of ATP-binding cassette (ABC) transporters has been widely reported in chemoradiotherapy resistance,<sup>42,43</sup> and MB et al. found that ABCC2 was co-expressed with stem cell markers.<sup>44</sup> CCR2 is a chemokine that specifically mediates monocyte chemotaxis. A recent study has indicated that CCR2 is significantly associated with immune infiltration and metastasis of lung cancer.<sup>45</sup> All five genes could serve as independent prognostic factors in LUAD.

TMB is a novel clinical subtype and presents an excellent predictive ability for immunotherapy in various cancers.<sup>46,47</sup> Our results suggested that TSISig was significantly positively associated with TMB ( $p < 0.001$ ) and negatively associated with the immune score in LUAD patients, and patients with low TSISig and high TMB showed the best prognosis ( $p < 0.0001$ ). Denton et al. confirmed that cancer-associated fibroblasts (CAFs) could not only inhibit the migration of immune cells to the tumor microenvironment and suppress their function but could also maintain tumor stemness, thus promoting the occurrence of cancer.<sup>48</sup> Our enrichment analysis for immune cells showed that the high-TSISig group contained higher CAFs than the low-TSISig group. These results revealed that TSISig might function by directly coordinating tumor stemness and immune suppression. Immune checkpoint inhibitors for PD-1 have become a popular therapy because of a good response to them by tumor patients.<sup>49,50</sup> The discovery of PD-1 expression in melanoma stem cells suggested that PD-1 might play a role in regulating tumor stemness.<sup>51</sup> Our results showed that TSISig was negatively correlated with PD-1 expression and that patients with low TSISig and high PD-1

expression had the best prognosis, while those with high TSISig and low PD-1 expression exhibited the worst prognosis. Therefore, we assumed that the combination of TSISig and PD-1 might improve the predictive ability of TSISig or PD-1 for the response to immunotherapy. Then, ROC curve analysis in the two datasets treated with immunotherapy suggested that combination analysis of TSISig and PD-1 led to a better predictive ability for immunotherapy compared to TSISig or PD-1 alone. Meanwhile, the predictive ability of TSISig for the response to immunotherapy was much better than that of PD-1 or TMB. Additionally, TIDE analysis also revealed the feasibility and accuracy of TSISig in predicting the immune response. These results suggest that TSISig could serve as an excellent predictor of the response to immunotherapy in patients with LUAD.

CSCs can promote tumor growth, recurrence, and metastasis, and show resistance to chemotherapy and radiotherapy in numerous tumors.<sup>20,52,53</sup> Thiery et al. thought that these adverse reactions may be caused by tumor stemness activation and immunosuppression caused by CAFs.<sup>54</sup> Giancotti et al. found that PRC1 could promote prostate cancer metastasis by coordinating stemness and immune suppression.<sup>8</sup> In the current study, we tried to measure the predictive ability of TSISig for the response to radiotherapy and tumor relapse. A higher rate of response to radiotherapy was demonstrated in patients with low TSISig. The ROC curve showed that TSISig had a good predictive ability for the response to radiotherapy (AUC = 0.691). Moreover, we found that patients with high TSISig were more likely to have tumor recurrence. An AUC value of 0.636 indicated that TSISig could predict LUAD recurrence partly. Finally, potential inhibitors such as HDAC inhibitors, CDK inhibitors, and NFkB pathway inhibitors targeting TSISig were screened out by CMap analysis. A previous study showed that HDAC inhibitors could enhance the efficacy of immunotherapy for lung tumors by reversing immunosuppression.<sup>55</sup> Consistently, Pan et al. found that HDAC inhibitors could suppress migration and eliminate CSCs in uveal melanoma.<sup>56</sup> These results further confirmed that TSISig could well characterize tumor stemness and immune infiltration of LUAD. HDAC inhibitors might serve as specific drugs for TSISig.

In summary, our study constructed a five-gene signature (TSISig) based on tumor stemness and immune-related specific genes. TSISig could not only accurately predict the prognosis of patients with LUAD within 2 years, but it could also be regarded as a novel and feasible predictor of LUAD recurrence and the response to immunotherapy or radiotherapy. Patients with low TSISig were more inclined to benefit from immunotherapy or radiotherapy. HDAC could inhibit the development of LUAD by targeting TSISig.

## AUTHOR CONTRIBUTIONS

ZD, HJ S, and LZ H designed the idea; HJ S, JP Z, and LZ H collected and analyzed the data, and drafted the paper; HJ S, KJ W, and JJ S analyzed the data; LZ H, JP Z, and MX revised the final paper. All authors read and approved the final manuscript.

## ETHICAL APPROVAL

Not applicable.

## CONFLICT OF INTEREST

All authors declare that there is no conflict of interest.

## DATA AVAILABILITY STATEMENT

All data in this study are available the Gene Expression Omnibus (<https://www.ncbi.nlm.nih.gov/geo/>) and TCGA (<https://portal.gdc.cancer.gov/>).

## ORCID

Zhe Dong  <https://orcid.org/0000-0002-4048-2337>

## REFERENCES

- Schabath MB, Cote ML. Cancer progress and priorities: lung cancer. *Cancer Epidemiol Biomarkers Prev*. 2019;28:1563-1579.
- Bray F, Ferlay J, Soerjomataram I, et al. Global cancer statistics 2018: GLOBOCAN estimates of incidence and mortality worldwide for 36 cancers in 185 countries. *CA Cancer J Clin*. 2018;68:394-424.
- Coleman MP, Quaresma M, Berrino F, et al. Cancer survival in five continents: a worldwide population-based study (CONCORD). *Lancet Oncol*. 2008;9:730-756.
- Siegel RL, Miller KD, Jemal A. Cancer statistics, 2018. *CA Cancer J Clin*. 2018;68:7-30.
- Steven A, Fisher SA, Robinson BW. Immunotherapy for lung cancer. *Respirology*. 2016;21:821-833.
- Dawood S, Austin L, Cristofanilli M. Cancer stem cells: implications for cancer therapy. *Oncology*. 2014;28:1101-1107, 1110.
- Steinbichler TB, Dudás J, Skvortsov S, et al. Therapy resistance mediated by cancer stem cells. *Semin Cancer Biol*. 2018;53:156-167.
- Su W, Han HH, Wang Y, et al. The polycomb repressor complex 1 drives double-negative prostate cancer metastasis by coordinating stemness and immune suppression. *Cancer Cell*. 2019;36(2):139-155.e10.
- Paczulla AM, Rothfelder K, Raffel S, et al. Absence of NKG2D ligands defines leukaemia stem cells and mediates their immune evasion. *Nature*. 2019;572:254-259.
- Fang M, Li Y, Huang K, et al. IL33 promotes colon cancer cell stemness via JNK activation and macrophage recruitment. *Cancer Res*. 2017;77:2735-2745.
- Helmy KY, Patel SA, Nahas GR, et al. Cancer immunotherapy: accomplishments to date and future promise. *Ther Deliv*. 2013;4:1307-1320.
- Ajani JA, Song S, Hochster HS, et al. Cancer stem cells: the promise and the potential. *Semin Oncol*. 2015;42(Suppl 1):S3-17.
- Malta TM, Sokolov A, Gentles AJ, et al. Machine learning identifies stemness features associated with oncogenic dedifferentiation. *Cell*. 2018;173:338-354.e315.
- Yoshihara K, Shahmoradgoli M, Martínez E, et al. Inferring tumour purity and stromal and immune cell admixture from expression data. *Nat Commun*. 2013;4:2612.
- Zeng LU, Fan X, Wang X, et al. Bioinformatics analysis based on multiple databases identifies hub genes associated with hepatocellular carcinoma. *Curr Genomics*. 2019;20:349-361.
- Zhang C, Chen T, Li Z, et al. Depiction of tumor stemlike features and underlying relationships with hazard immune infiltrations based on large prostate cancer cohorts. *Brief Bioinform*. 2021;22(3):bbaa211.
- Lamb J. The Connectivity Map: a new tool for biomedical research. *Nat Rev Cancer*. 2007;7:54-60.
- Liu SY, Wu YL. Ongoing clinical trials of PD-1 and PD-L1 inhibitors for lung cancer in China. *J Hematol Oncol*. 2017;10:136.
- Paulson KG, Lahman MC, Chapuis AG, et al. Immunotherapy for skin cancer. *Int Immunol*. 2019;31:465-475.
- Chang JC. Cancer stem cells: role in tumor growth, recurrence, metastasis, and treatment resistance. *Medicine*. 2016;95:S20-25.
- Battle E, Clevers H. Cancer stem cells revisited. *Nat Med*. 2017;23:1124-1134.
- Nassar D, Blanpain C. Cancer stem cells: basic concepts and therapeutic implications. *Annu Rev Pathol*. 2016;11:47-76.
- O'Brien CA, Pollett A, Gallinger S, et al. A human colon cancer cell capable of initiating tumour growth in immunodeficient mice. *Nature*. 2007;445:106-110.
- Leon G, MacDonagh L, Finn SP, et al. Cancer stem cells in drug resistant lung cancer: targeting cell surface markers and signaling pathways. *Pharmacol Ther*. 2016;158:71-90.
- Liu K, Xu SH, Chen Z, et al. TRPM7 overexpression enhances the cancer stem cell-like and metastatic phenotypes of lung cancer through modulation of the Hsp90alpha/uPA/MMP2 signaling pathway. *BMC Cancer*. 2018;18:1167.
- Papadaki MA, Stoupis G, Theodoropoulos PA, et al. Circulating tumor cells with stemness and epithelial-to-mesenchymal transition features are chemoresistant and predictive of poor outcome in metastatic breast cancer. *Mol Cancer Ther*. 2019;18:437-447.
- Xu M, Fang S, Song J, et al. CPEB1 mediates hepatocellular carcinoma cancer stemness and chemoresistance. *Cell Death Dis*. 2018;9:957.
- Faiao-Flores F, Smalley KSM. Get with the program! stemness and reprogramming in melanoma metastasis. *J Invest Dermatol*. 2018;138:10-13.
- Miranda A, Hamilton PT, Zhang AW, et al. Cancer stemness, intratumoral heterogeneity, and immune response across cancers. *Proc Natl Acad Sci USA*. 2019;116:9020-9029.
- Samstein RM, Lee C-H, Shoushtari AN, et al. Tumor mutational load predicts survival after immunotherapy across multiple cancer types. *Nat Genet*. 2019;51:202-206.
- Guo D, Wang M, Shen Z, et al. A new immune signature for survival prediction and immune checkpoint molecules in lung adenocarcinoma. *J Transl Med*. 2020;18:123.
- Sun S, Guo W, Wang Z, et al. Development and validation of an immune-related prognostic signature in lung adenocarcinoma. *Cancer Med*. 2020;9(16):5960-5975.
- Zhang Y, Fan Q, Guo Y, et al. Eight-gene signature predicts recurrence in lung adenocarcinoma. *Cancer Biomark*. 2020;28:447-457.
- Kim J, Hu Z, Cai L, et al. CPS1 maintains pyrimidine pools and DNA synthesis in KRAS/LKB1-mutant lung cancer cells. *Nature*. 2017;546:168-172.

35. Ghalamfarsa G, Kazemi MH, Raoofi Mohseni S, et al. CD73 as a potential opportunity for cancer immunotherapy. *Expert Opin Ther Targets*. 2019;23:127-142.
36. Pancione M, Giordano G, Remo A, et al. Immune escape mechanisms in colorectal cancer pathogenesis and liver metastasis. *J Immunol Res*. 2014;2014:1-11.
37. Allard B, Longhi MS, Robson SC, et al. The ectonucleotidases CD39 and CD73: novel checkpoint inhibitor targets. *Immunol Rev*. 2017;276:121-144.
38. Zhu J, Zeng Y, Li W, et al. CD73/NT5E is a target of miR-30a-5p and plays an important role in the pathogenesis of non-small cell lung cancer. *Mol Cancer*. 2017;16:34.
39. Zhou W, Wang Z, Shen NI, et al. Knockdown of ANLN by lentivirus inhibits cell growth and migration in human breast cancer. *Mol Cell Biochem*. 2015;398:11-19.
40. Xu J, Zheng H, Yuan S, et al. Overexpression of ANLN in lung adenocarcinoma is associated with metastasis. *Thorac Cancer*. 2019;10:1702-1709.
41. Olakowski M, Tyszkiewicz T, Jarzab M, et al. NBL1 and anillin (ANLN) genes over-expression in pancreatic carcinoma. *Folia Histochem Cytobiol*. 2009;47:249-255.
42. Qian C-Y, Zheng YI, Wang Y, et al. Associations of genetic polymorphisms of the transporters organic cation transporter 2 (OCT2), multidrug and toxin extrusion 1 (MATE1), and ATP-binding cassette subfamily C member 2 (ABCC2) with platinum-based chemotherapy response and toxicity in non-small cell lung cancer patients. *Chin J Cancer*. 2016;35:85.
43. Treenert A, Areepium N, Tanasanvimon S. Effects of ABCC2 and SLCO1B1 polymorphisms on treatment responses in Thai metastatic colorectal cancer patients treated with irinotecan-based chemotherapy. *Asian Pac J Cancer Prev*. 2018;19:2757-2764.
44. Duz MB, Karatas OF. Expression profile of stem cell markers and ABC transporters in 5-fluorouracil resistant Hep-2 cells. *Mol Biol Rep*. 2020;47:5431-5438.
45. Schmall A, Al-tamari HM, Herold S, et al. Macrophage and cancer cell cross-talk via CCR2 and CX3CR1 is a fundamental mechanism driving lung cancer. *Am J Respir Crit Care Med*. 2015;191:437-447.
46. Chan TA, Yarchoan M, Jaffee E, et al. Development of tumor mutation burden as an immunotherapy biomarker: utility for the oncology clinic. *Ann Oncol*. 2019;30:44-56.
47. Shrestha R, Prithviraj P, Anaka M, et al. Monitoring immune checkpoint regulators as predictive biomarkers in hepatocellular carcinoma. *Front Oncol*. 2018;8:269.
48. Denton AE, Roberts EW, Fearon DT. Stromal cells in the tumor microenvironment. *Adv Exp Med Biol*. 2018;1060:99-114.
49. Topalian SL, Drake CG, Pardoll DM. Immune checkpoint blockade: a common denominator approach to cancer therapy. *Cancer Cell*. 2015;27:450-461.
50. Wu X, Gu Z, Chen Y, et al. Application of PD-1 blockade in cancer immunotherapy. *Comput Struct Biotechnol J*. 2019;17:661-674.
51. Schatton T, Schütte U, Frank NY, et al. Modulation of T-cell activation by malignant melanoma initiating cells. *Cancer Res*. 2010;70:697-708.
52. Najafi M, Mortezaee K, Majidpoor J. Cancer stem cell (CSC) resistance drivers. *Life Sci*. 2019;234:116781.
53. Lyakhovich A, Leonart ME. Bypassing mechanisms of mitochondria-mediated cancer stem cells resistance to chemo- and radiotherapy. *Oxid Med Cell Longev*. 2016;2016:1716341.
54. Ma Q, Long W, Xing C, et al. Cancer stem cells and immunosuppressive microenvironment in glioma. *Front Immunol*. 2018;9:2924.
55. Topper MJ, Vaz M, Chiappinelli KB, et al. Epigenetic therapy ties MYC depletion to reversing immune evasion and treating lung cancer. *Cell*. 2017;171(6):1284-1300.e21.
56. Dai W, Zhou J, Jin B, et al. Class III-specific HDAC inhibitor Tenovin-6 induces apoptosis, suppresses migration and eliminates cancer stem cells in uveal melanoma. *Sci Rep*. 2016;6:22622.

## SUPPORTING INFORMATION

Additional supporting information may be found in the online version of the article at the publisher's website.

**How to cite this article:** Shi H, Han L, Zhao J, et al. Tumor stemness and immune infiltration synergistically predict response of radiotherapy or immunotherapy and relapse in lung adenocarcinoma. *Cancer Med*. 2021;10:8944-8960. doi:[10.1002/cam4.4377](https://doi.org/10.1002/cam4.4377)